



## Structure and reaction pathways of octanoic acid on copper

Robert Bavisotto, Resham Rana, Nicholas Hopper, Wilfred T Tysoe <sup>\*</sup>

Department of Chemistry and Biochemistry, University of Wisconsin-Milwaukee, Milwaukee, WI 53211, USA



### ARTICLE INFO

**Keywords:**

Octanoic acid  
Cu(100)  
Temperature-programmed desorption  
Infrared spectroscopy  
Density functional theory calculations  
Scanning tunneling microscopy

### ABSTRACT

The surface chemistry of octanoic acid was studied on a copper foil or a Cu(100) single crystal in ultrahigh vacuum using reflection-absorption infrared spectroscopy, temperature-programmed desorption, and supplemented by first-principles density functional theory (DFT) calculations. Octanoic acid adsorbs molecularly at 90 K, converting from a flat-lying species at low coverages to a more upright species at saturation. Adsorption at 300 K results in the formation of an  $\eta^2$ -octanoate species, which binds with the alkyl group parallel to the surface with a tilted carboxylate group, as evidence by both infrared data and calculations. The flat-lying structure facilitates octanoate decomposition, which reacts by desorbing carbon dioxide at  $\sim$ 550 K. Increasing the octanoate coverage induces the alkyl chains to be more perpendicular to the surface to form a self-assembled monolayer with significant intermolecular van der Waals' interactions. This stabilizes the adsorbate, which now decomposes by desorbing carbon dioxide at  $\sim$ 640 K, where infrared spectroscopy confirms that this also occurs by the carboxylate tilting towards the surface. The resulting heptyl species can either decompose by desorbing hydrogen or can also polymerize on the surface.

### 1. Introduction

Self-assembled monolayers (SAMs) [1–7] and, in particular, long-chain carboxylic acids have been used as so-called boundary lubricants [8–12], which bind strongly to the surface to prevent adhesion between the contacting interfaces, thereby lowering friction [13]. At high enough loads, carboxylic acids can tribochemically decompose under shear to form a lubricious, carbon-containing film [14–17]. Because it is challenging to study the surface chemistry occurring at a solid-solid interface to provide experimental information on the reaction pathways, it is often necessary to resort to theoretical methods to provide insights into the tribo/mechanochemistry. Thus, the mechanism of this tribochemical reaction has been investigated using molecular dynamics (MD) simulations of carboxylic acids that contain vinyl groups located at various positions in the chain. The results of the simulations suggest that vinyl-group containing carboxylic acids can simultaneously bind to both faces of the contact, resulting in very high forces being exerted on the linked molecule to induce it to tribochemically decompose. Of particular interest is that the *cis* and *trans* conformations of these carboxylic acids show different tribochemical activities, presumably because of steric constraints [18].

Recently it has become possible to investigate the reaction pathways at the solid-solid interface in ultrahigh vacuum [19–30] by measuring

the friction forces and the gas-phase species evolved while rubbing, and by monitoring the surface using Auger spectroscopy. These studies are facilitated by comparing the results with the thermal chemistry and by using first-principles density functional theory (DFT) calculations to gain insights into the surface reaction pathways and their energetics. Of relevance to studying the surface chemistry of longer-chain fatty acids, we have studied the shear-induced tribochemistry of acetic acid on copper [31], which has been shown previously to bind to the surface by forming a carboxylate species [32,33] with the methyl-carboxylate bond being normal to the surface [31]. The acetate species thermally decompose on copper by the plane of the acetate species tilting towards the surface and reacting to form adsorbed methyl species and evolve carbon dioxide gas when the temperature reaches  $\sim$ 590 K. This pathway was confirmed by DFT with a calculated activation energy that was in good agreement with experiment [31]. This reaction rate is tribologically accelerated by sliding so that a reaction that is thermally induced at  $\sim$ 590 K, now occurs at 300 K. However, since the acetate species are randomly azimuthally oriented on the surface, forces not only act in a direction perpendicular to the plane of the adsorbed acetate to push it towards the lowest-energy transition state, but can also be directed within the acetate plane. This induces the  $\eta^2$ -acetate species to also tilt, but to now form an  $\eta^1$ -acetate. The activation barrier for acetate decomposition via this pathway is slightly higher than that for the

\* Corresponding author.

E-mail address: [wtt@uwm.edu](mailto:wtt@uwm.edu) (W.T. Tysoe).

lowest-energy mechanism and the  $\eta^1$ -acetate decomposes to form carbon monoxide and adsorbed oxygen.

Similar surface chemistry experiments on longer-chain carboxylates will provide insights into the influence of vinyl groups in the chain and test the “molecular bridging” hypothesis outlined above. The thermal chemistry of 7-octenoic acid has been studied on copper using a combination of reflection-absorption infrared spectroscopy (RAIRS), X-ray photoelectron spectroscopy (XPS), temperature-programmed desorption (TPD) and scanning tunneling microscopy (STM). The analysis of the results was facilitated using first-principles density functional theory (DFT) calculations [34]. In addition, some previous work has also been carried out on other carboxylic acids adsorbed on copper using near-edge X-ray adsorption spectroscopy (NEXAFS) on Cu(111), where the structure was found to depend on the chain length [35,36]. The deprotonation kinetics of carboxylic acids on copper have been investigated by using fluorine-modified chains [37] and studies of the decomposition of isotopically labeled carboxylic acids have shown that the reaction is initiated by the removal of carbon dioxide from the carboxylate group [38].

The following investigates the adsorption of an alkyl-terminated carboxylic acid, octanoic acid, on a clean and annealed copper foil, supplemented by STM experiments on Cu(100). A copper foil, rather than a single crystal, was chosen as the substrate because tribological experiments will subsequently be carried out on this sample. Rubbing causes surface damage so that the use of single crystals is prohibitively expensive. However, it has been shown that these cleaned and vacuum annealed copper foils exhibit sufficient order to display distinct (100) low-energy electron diffraction (LEED) patterns [39].

## 2. Experimental methods

Experiments were carried out in UHV chambers operating at base pressures of  $\sim 2.0 \times 10^{-10}$  Torr after bakeout. Infrared spectra were collected using a Bruker Vertex 70 infrared spectrometer using a liquid-nitrogen-cooled, mercury cadmium telluride detector as described previously [40]. The surface was exposed to octanoic acid using a Knudsen source prior to collecting the infrared spectra. Temperature-dependent infrared experiments were performed by precisely controlling the sample temperature [34], which was monitored by means of a chromel/alumel thermocouple attached to the edge of the copper foil. The effective heating rate for these experiments was  $\sim 0.08$  K/s and thus enabled infrared spectra to be collected continuously under almost isothermal conditions. TPD experiments were carried out using a Dycor M200M quadrupole mass spectrometer as described previously [34]. The foil was dosed using various exposures of octanoic acid at 300 K and temperature was ramped at a rate of 5 K/second for each experiment. Octanoic acid coverages were measured from carbon/copper peak-to-peak ratios in Auger electron spectroscopy (AES).

The copper foil sample was prepared by mechanically polishing using sandpapers of increasingly fine grit until flat. This was followed by polishing using polycrystalline diamond paste in descending size until 1  $\mu$ m and resulted in a visibly smooth surface under a microscope. The foil was cleaned using a standard procedure that consisted of  $\text{Ar}^+$  bombardment with subsequent annealing to 850 K for 10 min.  $\text{Ar}^+$  bombardment was performed at a background gas pressure of  $\sim 3.0 \times 10^{-5}$  Torr at a 2 kV potential, while maintaining a  $\sim 2 \mu\text{A}$  sample current. The Cu(100) single crystal used in the STM experiments was cleaned by  $\text{Ar}^+$  bombardment for 30 min. This was followed by annealing at 875 K for 30 min. This cleaning procedure was repeated until the sample was found to be clean by AES.

Octanoic acid (Sigma-Aldrich Chemicals,  $\geq 99\%$  purity) was purified using several freeze-pump-thaw cycles and its cleanliness was judged by mass spectroscopy. Molecules were dosed using a Knudsen source with an attached tube of 3.2 mm internal diameter placed in close proximity ( $\sim 3$  cm) to the front of the sample. Exposures reported in this study are in units of Langmuirs ( $1 \text{ L} = 1 \times 10^{-6}$  Torr s) and the exposure values

were not corrected for ionization gauge sensitivities.

The octanoic acid binding structures were calculated using periodic density functional theory (DFT) using the projector augmented wave (PAW) method as implemented in the Vienna ab-initio simulation package (VASP) code [41–43]. The exchange and correlation energies were calculated using the PBE3 (Perdew, Burke and Ernzerhof [44]) form of the generalized gradient approximation (GGA). The kinetic energy cutoff for all calculations was 400 eV. The wavefunctions and electron density were converged to within  $1 \times 10^{-5}$  eV whereas geometric structures were optimized until the forces on the atoms were less than 0.01 eV/Å. Van der Waals interactions were implemented using the DFT-D3 method as described by Grimme et al [45]. The Brillouin zone was sampled using a  $\Gamma$ -centered Monkhorst-Pack ( $6 \times 6 \times 1$ ) k-point mesh for ( $2 \times 2$ ) unit cell structures, ( $3 \times 3 \times 1$ ) for ( $4 \times 4$ ) structures, and ( $2 \times 2 \times 1$ ) for the ( $6 \times 6$ ) structures. The surfaces were separated by 29 Å and the bottom two copper layers were kept frozen for all calculations. The Cu(100) lattice constant used was 3.63 Å.

## 3. Results

Surface analyses of octanoic acid were performed on an annealed copper foil using RAIRS, TPD, and by STM on a Cu(100) single crystal. RAIRS experiments were carried out by exposing a polished copper foil to octanoic acid at 90 K and the results are displayed in Fig. 1A as a

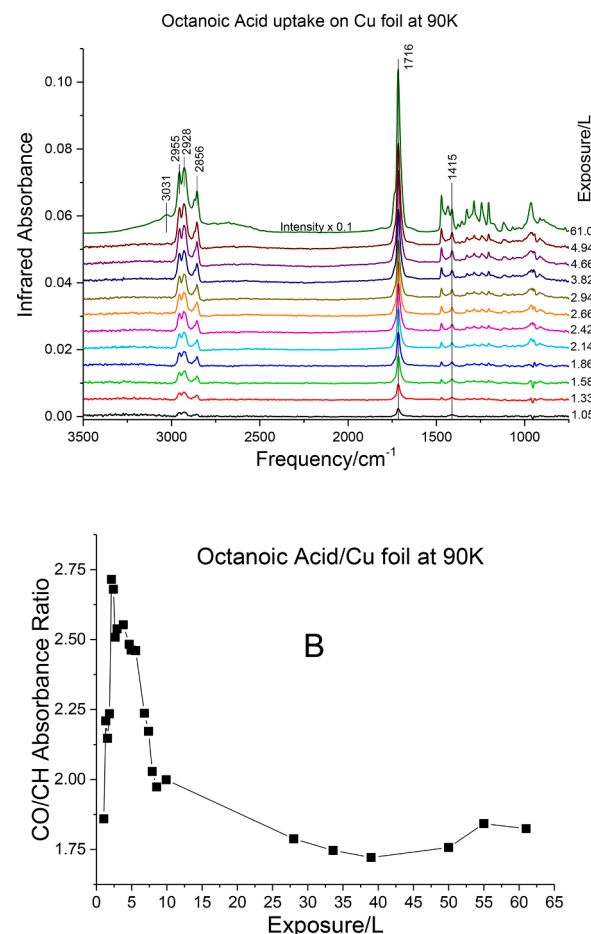


**Fig. 1.** (A) Infrared spectra collected using a resolution of  $4 \text{ cm}^{-1}$  for the adsorption of octanoic acid on Cu(100) at a sample temperature of 90 K as a function of exposure on Langmuirs (L), where the exposures are displayed adjacent to the corresponding spectrum. (B) The ratio of the integrated absorbances of the CO and CH modes as a function of exposure, in Langmuirs (L). The statistical measurement errors in the ratios are  $\sim 1\%$  of the signals and are within the size of the symbols on the graph.

function of exposure, where the exposures (in Langmuirs) are displayed adjacent to the corresponding spectra. At low exposures, the observed vibrational frequencies are assigned as follows:  $1716\text{ cm}^{-1}$  (carbonyl mode),  $1415\text{ cm}^{-1}$  (O-H bending vibration), CH stretching modes at  $2955$ ,  $2928$  and  $2856\text{ cm}^{-1}$ . The presence of the O-H bending vibration indicates that octanoic acid adsorbed on copper at low temperatures remains in its molecular form [46]. At higher coverages, a broad feature appears between  $2500$  and  $3200\text{ cm}^{-1}$  and indicates the formation of hydrogen-bonded dimers between neighboring COOH groups [47]. The ratios of the integrated absorbances of the octanoic acid CO and CH modes are plotted in Fig. 1B. This ratio increase rapidly at the lowest coverages from  $\sim 1.75$  for initial adsorption to a value of  $2.75$  at an exposure  $\sim 2.1$  to  $3.8\text{ L}$ . The ratio slowly decreases with increasing exposure to a plateau at a value of  $\sim 1.75$  for exposures larger than  $28\text{ L}$ . Previous work on 7-octenoic acid on copper shows similar behavior, with a peak in the plot of the ratio of CO to CH modes reaching a maximum at  $\sim 2\text{ L}$  [34], corresponding to the completion of the first monolayer.

The effect of heating the octanoic acid multilayer formed by an exposure of  $61\text{ L}$ , corresponding to a multilayer for  $\sim 30\text{ ML}$  thick, is shown in Fig. 2A, where the annealing temperatures are displayed adjacent to the corresponding spectra. The carbonyl stretching modes are shown in Fig. 2B and the peak positions remain unchanged as the sample is heated up to  $169\text{ K}$ . Upon annealing to  $180\text{ K}$ , the carbonyl vibrations sharpen and shift to lower frequency. This shift is

accompanied by sharpening of the CH stretching modes between  $2800$  and  $3000\text{ cm}^{-1}$  (Fig. 2C) and the appearance of a sharp peak at  $939\text{ cm}^{-1}$  (Fig. 2A). The broad OH mode between  $3200\text{ cm}^{-1}$  and  $2500\text{ cm}^{-1}$  starts to disappear over this temperature range. These changes indicate that the multilayer is becoming more ordered as the dimers dissociate at higher temperatures. The loss of intensity of all IR modes when annealing to temperatures above  $246\text{ K}$  indicate that the multilayer has begun desorption. The spectrum obtained by heating to  $251\text{ K}$  shows a broad OH peak at  $3215\text{ cm}^{-1}$ , indicating that the remaining surface-bound monolayer octanoic acid has a portion of its species that has not been deprotonated. The peaks at  $1425$  and  $1408\text{ cm}^{-1}$  are assigned to adsorbed carboxylate groups [31,32,34] and indicate that a portion of the octanoic acid deprotonates on the surface and the surface infrared section rules [48], which indicate that only modes with a vibrational component perpendicular to the surface are detected, show that the COO group has a component of the vibration that is perpendicular to surface.

The infrared spectra obtained for octanoic acid adsorbed on copper at  $300\text{ K}$  are shown in Fig. 3A. The peak centered at  $1423\text{ cm}^{-1}$  is assigned to the COO symmetric stretching mode. The variation in the integrated intensities of the COO ( $\blacktriangle$ ) and CH<sub>2</sub> stretching modes ( $\blacksquare$ ,  $\bullet$ ) is plotted versus exposure in Langmuirs in Fig. 3B. The resulting integrated absorbance ratios are shown in Fig. 3C. The surface infrared section rules [48] indicate that the observed intensity variation implies that there is a change in molecular orientation as the coverage increases with exposure up to  $\sim 2\text{ L}$ . This is taken to correspond to the octanoic acid exposure that saturates the copper surface and the COO vibrational frequency at this coverage ( $1425\text{ cm}^{-1}$ ) is close to that found for bidentate acetate species on Cu(100) [31,32], indicating that octanoic acid also deprotonates and binds to the surface as a bidentate carboxylate.

The effects of heating the octanoate monolayer on copper are investigated by RAIRS (Fig. 4A) and TPD obtained by monitoring  $44\text{ amu}$  (Fig. 4B, CO<sub>2</sub>) and  $2\text{ amu}$  (Fig. 4C, H<sub>2</sub>) at a heating rate of  $5\text{ K/second}$ . The RAIR spectra were collected continuously at a rate of  $0.08\text{ K/second}$ . The relative coverages for the TPD experiments were estimated from the C(KLL)/O(KLL) peak-to-peak Auger ratios normalized to the ratio at saturation. Fig. 4A shows the temperature dependence of the  $1425\text{ cm}^{-1}$  feature (COO<sub>sym</sub> stretch) and the corresponding appearance of the  $1490\text{ cm}^{-1}$  peak (COO<sub>asym</sub> stretch), which commences by  $415\text{ K}$ . The infrared surface selection rules [48] indicate that the change in ratio of these modes is due to the octanoate species starting to tilt towards the surface.

Fig. 4B shows an intense  $44\text{ amu}$  (CO<sub>2</sub>) peak that is centered at  $645\text{ K}$  indicating thermally-induced decarboxylation of the adsorbed octanoate species. A small shoulder at lower temperatures (centered at  $525\text{ K}$ ) is evidence that decarboxylation is facilitated at low octanoate coverages. A  $2\text{ amu}$  peak (Fig. 4C), with a main feature that is also centered at  $645\text{ K}$ , grows with increasing coverage. This indicates that the resulting heptyl group decomposes rapidly once it is formed. As the coverage approaches saturation, an additional, higher-temperature shoulder appears centered at  $700\text{ K}$ , as well as a lower-temperature peak centered at  $570\text{ K}$ .

Fig. 5 shows STM images of the saturated octanoic acid monolayer on copper after heating to  $850\text{ K}$  and cooling to  $300\text{ K}$  to collect the images. It is observed that the octanoic acid forms polymer-like decomposition products on the Cu(100) surface, similar to those found previously for the decomposition of 7-octenoic acid on copper [34]. These polymers are present not only on the terraces, but also appear to agglomerate towards step edges as illustrated in Fig. 5 by black arrows. It is also observed that these polymer-like products have large regions that could be forming macrocyclic products or folded alkyl chains as illustrated by white circles in Fig. 5. Fig. 5C and D are scans of the same area taken  $17\text{ minutes}$  apart showing that the carbonaceous overlayers are very stable on the surface.

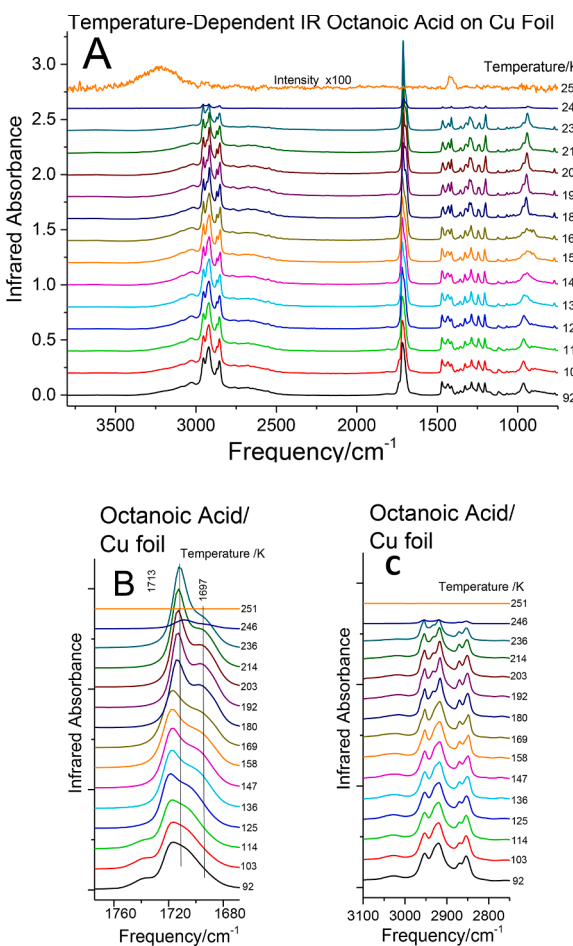
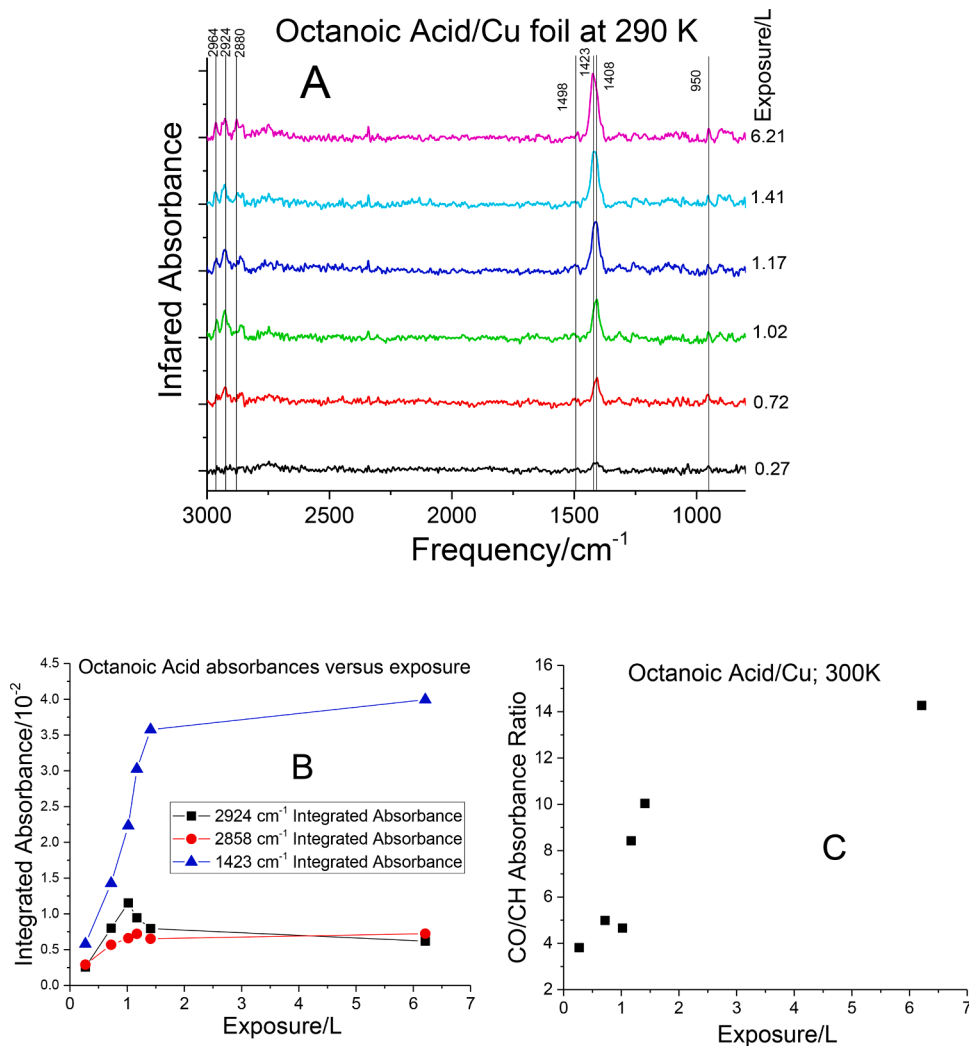


Fig. 2. (A) Infrared spectra collected using a resolution of  $4\text{ cm}^{-1}$  for the adsorption of octanoic acid on Cu(100) at a sample temperature of  $90\text{ K}$  heated to various temperatures, where the temperatures are displayed adjacent to the corresponding spectrum. (B) Spectra showing the carbonyl modes and (D) Spectra showing the CH mode stretching modes in greater detail.



**Fig. 3.** (A) Infrared spectra collected using a resolution of  $4\text{ cm}^{-1}$  for the adsorption of octanoic acid on Cu(100) at a sample temperature of 300 K as a function of exposure on Langmuirs (L), where the exposures are displayed adjacent to the corresponding spectrum. (B) Plot of the integrated absorbances for the carbonyl mode (CO vibration at  $\sim 1711\text{ cm}^{-1}$ ) and the C–H stretching vibrations (CH vibrations at  $\sim 2930\text{ cm}^{-1}$ ) and as a function of the octanoic acid exposure and (C), the ratio of the integrated absorbances of the CO and CH modes as a function of exposure, in Langmuirs (L). The statistical measurement errors in the ratios are  $\sim 1\%$  of the signals and are within the size of the symbols on the graphs.

#### 4. Discussion

DFT calculations were carried out to assist in analyzing the experimental results and the low-coverage structure is depicted in Fig. 6, where Fig. 6A shows the side view and Fig. 6B shows the top view of the adsorbed octanoate and illustrates that large intermolecular spacing used in the calculation. This shows that the most-stable, low-coverage configuration is when the alkyl chain interacts with the copper surface via van der Waals' interactions to lie parallel to the surface. This causes the plane of the carboxylate to tilt to enable the chain to access the surface. Note that the resulting in-plane tilting of the carboxylate group leads to carboxylate decomposition and the evolution of carbon dioxide and the deposition of only carbon on the surface [31,33]. The heat of adsorption measured from the difference in energy of the adsorbate plus the substrate and the sum of the energies of the clean slab and the isolated molecule is  $-398\text{ kJ/mol}$ . This indicates that the van der Waals' surface interactions are relatively strong [26].

Figs. 7 A to C show the octanoate structures at higher coverages with the COO plane oriented perpendicular to the surface. Because of the tetrahedral structure around the carbon, this leads to a tilted alkyl chain and a low-coverage binding energy (Fig. 7C) of  $-350\text{ kJ/mol}$  (Fig. 7D). This indicates that the flat-lying species is more stable than the upright one on copper so that the energy penalty due to tilting of the COO anchoring group is compensated for by the van der Waals' interactions with the surface. The adsorption energy for 7-octenoic acid, which has the same number of carbons as octanoic acid but has a terminal vinyl

group, is  $\sim 411\text{ kJ/mol}$  so that the  $\pi$ -orbital binding to copper is only slightly stronger than the alkyl van der Waals interactions. Increasing the octanoate coverage strengthens the binding due to interchain van der Waals' interactions with the surface to form a SAM (Fig. 7C).

Infrared spectroscopy indicates that octanoic acid adsorbs as an intact molecule at 90 K, with a spectrum that is in agreement with that of the frequencies found for liquid octanoic acid at all coverages (Fig. 1A). There are, however, changes in the relative intensities of the infrared features as indicated in Fig. 1B, where the intensity of the carbonyl vibration relative the CH stretching modes depends on the exposure and increases to reach a maximum between 2.1 and 3.8 L. Since the CH vibrations are predominantly due to the methylene stretching modes, which vibrate perpendicularly to the chain, while the carbonyl will have a component parallel to the chain, the changes in relative intensity connote a change in molecular orientation. This indicates that octanoic acid lies close to flat to the surface at lower coverage, and becomes more perpendicular as the coverage increases to saturate the first monolayer to form a SAM at between 2.1 and 3.8 L. By definition, multilayers form at higher exposures so that molecules become more randomly ordered within the film, thereby causing a decrease in the CO/CH absorbance ratio.

The effect of heating this molecular layer is shown in Fig. 2A, where the carbonyl stretches are displayed in Fig. 2B and the CH modes in Fig. 2C, as a function of temperature. Annealing the thin films causes it to order so that the environment around each molecule is much more uniform to cause the peaks to sharpen and the CO/CH intensity ratio to

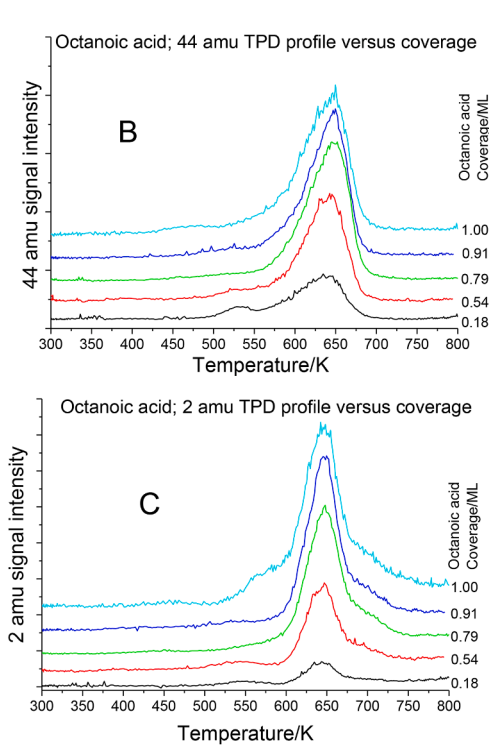
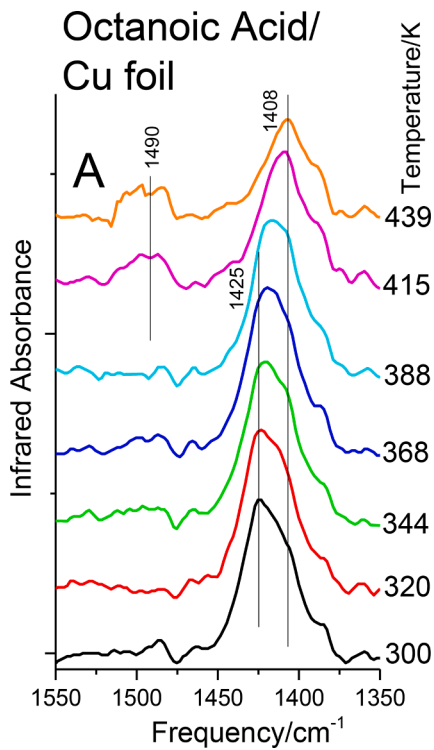


**Fig. 4.** (A) Infrared spectra collected using a resolution of  $4\text{ cm}^{-1}$  for the adsorption of octanoic acid on Cu(100) at a sample temperature of 300 K heated to various temperatures, where the temperatures are displayed adjacent to the corresponding spectrum. (B) Temperature-programmed desorption (TPD) profiles for the adsorption of octanoic acid on Cu(100) at a sample temperature of 300 K as a function of octanoic coverage using a heating rate of 5 K/s while monitoring (B) 44 and (C) 2 amu, where coverages are displaced adjacent to the corresponding spectrum.

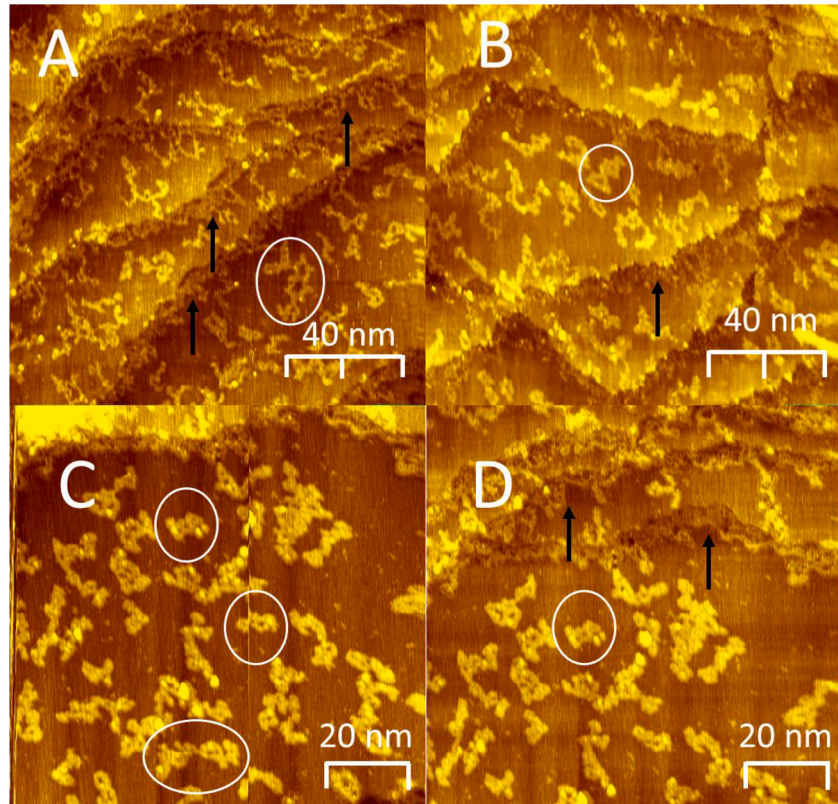


**Fig. 5.** Scanning tunnel microscope (STM) images of a saturated overlayer of octanoic acid adsorbed at 300 K on Cu(100). (A)  $150\text{ nm} \times 150\text{ nm}$  image after heating to 850 K ( $V_b = -0.75\text{ V}$ ,  $I_t = 0.083\text{ nA}$ ), (B)  $150\text{ nm} \times 150\text{ nm}$  image after heating to 850 K ( $V_b = -0.75\text{ V}$ ,  $I_t = 0.097\text{ nA}$ ) and (C)  $100\text{ nm} \times 100\text{ nm}$  image ( $V_b = -0.75\text{ V}$ ,  $I_t = 0.098\text{ nA}$ ) image after heating to 850 K, (D)  $100\text{ nm} \times 100\text{ nm}$  image ( $V_b = -0.75\text{ V}$ ,  $I_t = 0.097\text{ nA}$ ) of the same region taken 17 min after image C.

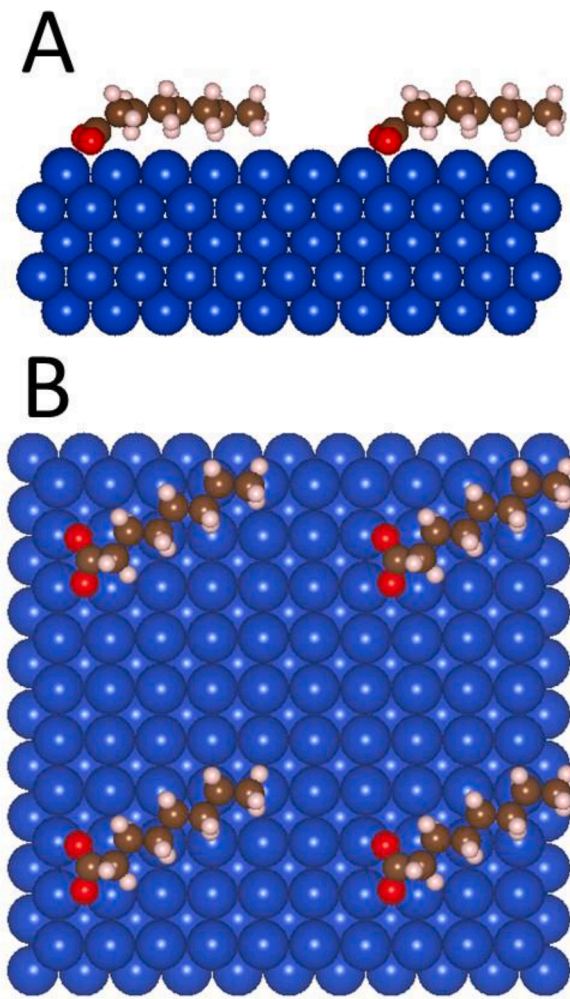


**Fig. 6.** Most-stable structure of flat-lying octanoic acid on Cu(100) calculated by density functional theory showing (A) a top view and (B) a side view.

increase. Heating to  $\sim 230$  K causes a large increase in the absorbance ratio connoting even greater order of the octanoic acid and there is evidence for some deprotonation on annealing to  $\sim 260$  K to create a COO surface linker group with a bidentate adsorption geometry.

Adsorption of octanoic acid at room temperature leads to the direct formation of octanoate species on the surface (Fig. 3A), where the overlayer saturates at  $\sim 2$  L. The integrated CO/CH intensity ratio changes as a function of octanoic acid exposure (Fig. 3C), in accord with the DFT prediction described above, where it forms flat-lying species at low coverage [5,49], evolving to a more perpendicular orientation at higher coverages. This tilt of the carboxylate group causes the asymmetric COO vibration to become infrared allowed [48] and to be detected at  $\sim 1498$   $\text{cm}^{-1}$ . The symmetric stretch also increases in intensity as the coverage increases, and shifts from  $\sim 1408$  to  $1423$   $\text{cm}^{-1}$  due to changes in the COO binding to the surface. When the exposure reaches  $\sim 1.4$  to  $6.2$  L, the peak due to the symmetric stretch has disappeared to leave only a mode at  $\sim 1423$   $\text{cm}^{-1}$ , close to the frequencies found for 7-octenoate ( $1425$   $\text{cm}^{-1}$ ) [34] and acetate ( $1437$   $\text{cm}^{-1}$ ) on copper [32,31].

The reverse effect is evident as the octanoate-covered surface is heated (Fig. 4A), where a  $\sim 1490$   $\text{cm}^{-1}$  peak appears as the sample is heated to  $\sim 440$  K, and the  $\sim 1425$   $\text{cm}^{-1}$  peak shifts to  $\sim 1408$   $\text{cm}^{-1}$ . This is ascribed to a dynamic tilting that occurs without any thermal decomposition (no species desorb at this temperature (see Figs. 4 B and C)). Similar effects are seen for 7-octenoic acid, which also tilts as the temperature increases [34]. This indicates that these short-chain

carboxylic acids are relatively dynamic on the surface. However, they do not appear to tilt sufficiently to induce decarboxylation until the temperature reaches  $\sim 530$  K, where some  $\text{CO}_2$  is detected at low coverages (Fig. 4B). However, only a small portion of  $\text{CO}_2$  is produced at  $\sim 530$  K at low coverages, and the remainder desorbs at  $\sim 640$  K in the major  $\text{CO}_2$  desorption state. This implies that the octanoate species are not uniformly distributed on the surface but rather form patches of crowded adsorbates that form a SAM, with lower-coverage regions with tilted species (Fig. 6) that can more easily decompose, while the more crowded patches react at  $\sim 640$  K.

Decarboxylation results in the evolution of carbon dioxide in states at  $\sim 530$  and  $640$  K to produce an adsorbed heptyl species. The surface chemistry of alkyl species has been studied on transition-metal surfaces [50], and copper in particular [51,52], by grafting them on the surface from iodine-containing precursors. The major decomposition pathway is a  $\beta$ -hydride elimination reaction that occurs at  $\sim 200$  to  $250$  K in TPD, and is many orders of magnitude faster than  $\alpha$ -hydride elimination processes. Coupling reactions can also occur at  $\sim 430$  K, so that hydride elimination and coupling reactions occur at much lower temperatures than the decarboxylation temperature ( $\sim 640$  K, Fig. 4B). This indicates that alkyl species are reactively formed in a highly vibrationally excited state. It is therefore expected that these alkyl decomposition reactions will occur rapidly, but with different reaction selectivities at higher temperatures where, by definition, the relative rates of processes that occur with higher activation energies will be higher. As an example, alkyl species primarily undergo  $\beta$ -hydride elimination, consistent with the desorption of hydrogen at  $\sim 550$  and  $640$  K indicating that decarboxylation is the rate-limiting step for the production of hydrogen in these states.

To investigate coupling processes, which in the case of octanoic acid would produce at least  $\text{C}_{14}$  chains, STM images were collected of the surface after reaction of adsorbed octanoic acid on Cu(100) at  $850$  K (Fig. 5). Figs. 5 A and B show low-magnification images and Fig. 5 C shows higher magnifications. This reveals the formation of polymer-like species but with chains length that are much longer than the value of  $\sim 2$  nm expected for  $\text{C}_{14}$  chains. There is a clear tendency for oligomers to nucleate and grow from step edges and the high-magnification images suggest either the formation of macrocyclic species or a closely packed group of folded alkyl chains. Fig. 5D shows the same regions as Fig. 5C, both collected at room temperature, but obtained  $17$  min apart. Apart from some image drift, the images are identical, confirming that the overlayers formed at high temperatures are stable and immobile at room temperature.

There is an additional low-temperature hydrogen formation pathway in a 2 amu peak centered at  $\sim 560$  K, but not accompanied by the production of  $\text{CO}_2$  that is evident for a saturated overlayer of octanoate species (Fig. 4 C). This must be due to dehydrogenation of the intact molecule, which could, of course, occur when the adsorbate tilts with the alkyl group to reaching the surface (Fig. 1). This is presumably least likely to occur for a saturated overlayer. The low-coverage theoretical results show that alkyl group interactions with the surface cause the carboxylate plane to tilt towards the surface, thus facilitating the decomposition pathway that leads to carbon dioxide formation.

## 5. Conclusions

The surface chemistry of octanoic acid is studied on a copper foil and Cu(100) single crystals in UHV after adsorption at  $90$  and  $300$  K to understand the surface structure and reaction pathways as a precursor to investigating the mechano- or tribochemical reaction pathways. The surface structure and reaction pathways are investigated using infrared spectroscopy and TPD, and the surface produced after high-temperature reaction is imaged by STM.

DFT calculations show that the carboxylate species lies flat on the surface at low coverages and this adsorbate geometry is confirmed using infrared spectroscopy. This indicates that the van der Waals' interaction

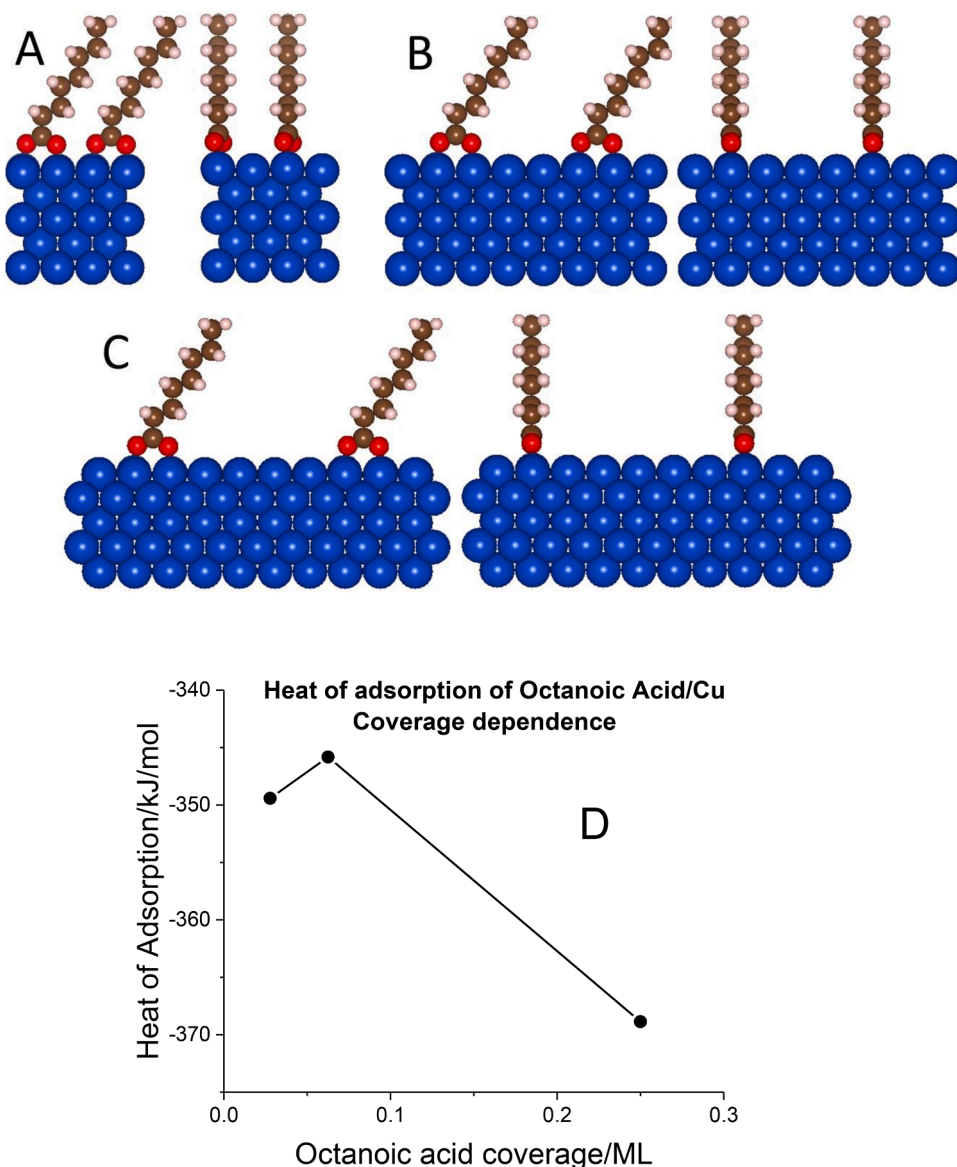


**Fig. 7.** Most-stable structure of vertical octanoic acid on Cu(100) calculated by density functional theory showing (A) a  $2 \times 2$ , (B) a  $4 \times 4$  and (C) a  $6 \times 6$  overlayer, and figure (D) shows the heat of adsorption of octanoic acid as a function of coverage.

between the chain and the surface is sufficiently strong to cause the carboxylate group to tilt towards the surface. Carboxylates react thermally by the carboxylate group tilting to evolve carbon dioxide, implying that low-coverage carboxylate overlayers should be reactive, as evidenced by carbon dioxide desorption at  $\sim 550$  K. This could be viewed as a mechanochemical process with the intermolecular forces between the hydrocarbon chain and the surface serving to accelerate the reaction.

As the octanoate coverage increases, surface crowding causes the octanoate to reorient so that the alkyl chains are more perpendicular to the surface, which causes the decomposition temperature to increase to  $\sim 640$  K, where the reaction also evolves carbon dioxide. This is accompanied by the synchronous desorption of hydrogen due to dehydrogenation of the reactively formed alky species, and the formation of polymeric species on the surface. Further evidence for the SAMs decomposing by the octanoate tilting towards the surface comes from the detection of asymmetric carbonyl stretching modes that, according to the surface infrared selection rules, can only appear when the carboxylate tilt.

#### Declaration of Competing Interest

The authors declare no conflict of interest.

#### Acknowledgements

We gratefully acknowledge the Civil, Mechanical and Manufacturing Innovation (CMMI) Division of the National Science Foundation under grant number CMMI-2020525 for support of this work.

#### References

- [1] H. Sellers, A. Ulman, Y. Shnidman, J.E. Eilers, Structure and binding of alkanethiolates on gold and silver surfaces: implications for self-assembled monolayers, *J. Am. Chem. Soc.* 115 (1993) 9389–9401.
- [2] J.I. Henderson, S. Feng, G.M. Ferrence, T. Bein, C.P. Kubiak, Self-assembled monolayers of dithiols, diisocyanides, and isocyanothiols on gold: ‘chemically sticky’ surfaces for covalent attachment of metal clusters and studies of interfacial electron transfer, *Inorg. Chim. Acta* 242 (1996) 115–124.
- [3] T. Ishida, S.I. Yamamoto, W. Mizutani, M. Motomatsu, H. Tokumoto, H. Hokari, H. Azebara, M. Fujihira, Evidence for cleavage of disulfides in the self-assembled monolayer on Au(111), *Langmuir* 13 (1997) 3261–3265.

[4] S.A. Swanson, R. McClain, K.S. Lovejoy, N.B. Alamdari, J.S. Hamilton, J.C. Scott, Self-assembled diisocyanide monolayer films on gold and palladium, *Langmuir* 21 (2005) 5034–5039.

[5] C. Vericat, M.E. Vela, R.C. Salvarezza, Self-assembled monolayers of alkanethiols on Au(111): surface structures, defects and dynamics, *PCCP* 7 (2005) 3258–3268.

[6] N.A. Kautz, S.A. Kandel, Alkanethiol/Au(111) self-assembled monolayers contain gold adatoms: scanning tunneling microscopy before and after reaction with atomic hydrogen, *J. Am. Chem. Soc.* 130 (2008) 6908–6909.

[7] D.P. Woodruff, The interface structure of n-alkylthiolate self-assembled monolayers on coinage metal surfaces, *PCCP* 10 (2008) 7211–7221.

[8] D. Clayton, An introduction to boundary and extreme pressure lubrication, *Br. J. Appl. Phys.* 2 (1951) 25.

[9] F.J. Westlake, A. Cameron, A study of ultra-thin lubricant films using an optical technique, proceedings of the institution of mechanical engineers, *Conference Proc.* 182 (1967) 75–78.

[10] A. Tonck, J.M. Martin, P. Kapsa, J.M. Georges, Boundary lubrication with anti-wear additives: study of interface film formation by electrical contact resistance, *Tribol. Int.* 12 (1979) 209–213.

[11] S.M. Hsu, R.S. Gates, Boundary lubricating films: formation and lubrication mechanism, *Tribol. Int.* 38 (2005) 305–312.

[12] H. Spikes, Friction modifier additives, *Tribol. Lett.* 60 (2015) 5.

[13] R. Simić, M. Kalin, Adsorption mechanisms for fatty acids on DLC and steel studied by AFM and tribological experiments, *Appl. Surf. Sci.* 283 (2013) 460–470.

[14] M. Kano, J.M. Martin, K. Yoshida, M.I. De Barros Bouchet, Super-low friction of ta-C coating in presence of oleic acid, *Friction* 2 (2014) 156–163.

[15] M.I. De Barros Bouchet, J.M. Martin, J. Avila, M. Kano, K. Yoshida, T. Tsuruda, S. Bai, Y. Higuchi, N. Ozawa, M. Kubo, M.C. Asensio, Diamond-like carbon coating under oleic acid lubrication: evidence for graphene oxide formation in superlow friction, *Sci. Rep.* 7 (2017) 46394.

[16] M.I. De Barros Bouchet, J.M. Martin, C. Forest, T. le Mogne, M. Mazarin, J. Avila, M.C. Asensio, G.L. Fisher, Tribocchemistry of unsaturated fatty acids as friction modifiers in (bio)diesel fuel, *RSC Adv.* 7 (2017) 33120–33131.

[17] S. Campen, J.H. Green, G.D. Lamb, H.A. Spikes, In situ study of model organic friction modifiers using liquid cell AFM; saturated and mono-unsaturated carboxylic acids, *Tribol. Lett.* 57 (2015) 18.

[18] T. Kuwahara, P.A. Romero, S. Makowski, V. Weihnacht, G. Moras, M. Moseler, Mechano-chemical decomposition of organic friction modifiers with multiple reactive centres induces superlubricity of ta-C, *Nat. Commun.* 10 (2019) 151.

[19] O.J. Furlong, B.P. Miller, W.T. Tysoe, Shear-induced surface-to-bulk transport at room temperature in a sliding metal–metal interface, *Tribol. Lett.* 41 (2011) 257–261.

[20] O.J. Furlong, B.P. Miller, P. Kotvis, W.T. Tysoe, Low-temperature, shear-induced tribofilm formation from dimethyl disulfide on copper, *ACS Appl. Mater. Interfaces* 3 (2011) 795–800.

[21] O. Furlong, B. Miller, W. Tysoe, Shear-induced surface-to-bulk transport at room temperature in a sliding metal–metal interface, *Tribol. Lett.* 41 (2011) 257–261.

[22] O. Furlong, B. Miller, W.T. Tysoe, Shear-induced boundary film formation from dialkyl sulfides on copper, *Wear* 274–275 (2012) 183–187.

[23] B.P. Miller, O.J. Furlong, W.T. Tysoe, Surface chemistry of isopropoxy tetramethyl dioxaborolane on Cu (111), *Langmuir* 28 (2012) 6322–6327.

[24] B.P. Miller, O.J. Furlong, W.T. Tysoe, The kinetics of shear-induced boundary film formation from dimethyl disulfide on copper, *Tribol. Lett.* 49 (2013) 39–46.

[25] B. Miller, P. Kotvis, O. Furlong, W. Tysoe, Relating molecular structure to tribological chemistry: borate esters on copper, *Tribol. Lett.* 49 (2013) 21–29.

[26] B. Miller, O.J. Furlong, W.T. Tysoe, The desorption and reaction of 1-alkenes and 1-alkynes on Cu(111) and copper foils, *Surf. Sci.* 616 (2013) 143–148.

[27] B. Miller, O. Furlong, W. Tysoe, Tribological properties of 1-alkenes on copper foils: effect of low-coordination surface sites, *Tribol. Lett.* 51 (2013) 357–363.

[28] B. Miller, O. Furlong, W. Tysoe, The kinetics of shear-induced boundary film formation from dimethyl disulfide on copper, *Tribol. Lett.* 49 (2013) 39–46.

[29] H. Adams, B.P. Miller, P.V. Kotvis, O.J. Furlong, A. Martini, W.T. Tysoe, In situ measurements of boundary film formation pathways and kinetics: dimethyl and diethyl disulfide on copper, *Tribol. Lett.* 62 (2016) 1–9.

[30] H. Adams, B.P. Miller, O.J. Furlong, M. Fantauzzi, G. Navarra, A. Rossi, Y. Xu, P. V. Kotvis, W.T. Tysoe, Modeling mechanochemical reaction mechanisms, *ACS Appl. Mater. Interfaces* 9 (2017) 26531–26538.

[31] R. Rana, R. Bavisotto, N. Hopper, W. Tysoe, Inducing high-energy-barrier tribocatalytic reaction pathways: acetic acid decomposition on copper, *Tribol. Lett.* 69 (2021) 32.

[32] B.A. Sexton, The structure of acetate species on copper (100), *Chem. Phys. Lett.* 65 (1979) 469–471.

[33] M. Bowker, R.J. Madix, The adsorption and oxidation of acetic acid and acetaldehyde on Cu(110), *Appl. Surface Sci.* 8 (1981) 299–317.

[34] R. Bavisotto, R. Rana, N. Hopper, D. Olson, W.T. Tysoe, Adsorption and reaction pathways of 7-octenoic acid on copper, *PCCP* 23 (2021) 5834–5844.

[35] D. Fuhrmann, D. Wacker, K. Weiss, K. Hermann, M. Witko, C. Wöll, The adsorption of small hydrocarbons on Cu(111): a combined He-atom scattering and x-ray absorption study for ethane, ethylene, and acetylene, *J. Chem. Phys.* 108 (1998) 2651–2658.

[36] M. Wühn, J. Weckesser, C. Wöll, Bonding and orientational ordering of long-chain carboxylic acids on Cu(111): investigations using X-ray absorption spectroscopy, *Langmuir* 17 (2001) 7605–7612.

[37] B. Immaraporn, P. Ye, A.J. Gellman, The transition state for carboxylic acid deprotonation on Cu(100), *J. Phys. Chem. B* 108 (2004) 3504–3511.

[38] B. Karagoz, A. Reinicker, A.J. Gellman, Kinetics and mechanism of aspartic acid adsorption and its explosive decomposition on Cu(100), *Langmuir* 35 (2019) 2925–2933.

[39] O.J. Furlong, B.P. Miller, Z. Li, J. Walker, L. Burkholder, W.T. Tysoe, The surface chemistry of dimethyl disulfide on copper, *Langmuir* 26 (2010) 16375–16380.

[40] M. Kaltchev, A.W. Thompson, W.T. Tysoe, Reflection-absorption infrared spectroscopy of ethylene on palladium (111) at high pressure, *Surf. Sci.* 391 (1997) 145–149.

[41] G. Kresse, J. Hafner, Ab initio molecular dynamics for liquid metals, *Phys. Rev. B* 47 (1993) 558–561.

[42] G. Kresse, J. Furthmüller, Efficiency of ab-initio total energy calculations for metals and semiconductors using a plane-wave basis set, *Comput. Mater. Sci.* 6 (1996) 15–50.

[43] G. Kresse, J. Furthmüller, Efficient iterative schemes for ab initio total-energy calculations using a plane-wave basis set, *Phys. Rev. B* 54 (1996) 11169–11186.

[44] J.P. Perdew, K. Burke, M. Ernzerhof, Generalized gradient approximation made simple, *Phys. Rev. Lett.* 77 (1996) 3865–3868.

[45] S. Grimme, J. Antony, S. Ehrlich, H. Krieg, A consistent and accurate ab initio parametrization of density functional dispersion correction (DFT-D) for the 94 elements H–Pu, *J. Chem. Phys.* 132 (2010), 154104.

[46] J.-J. Max, C. Chapados, Infrared spectroscopy of aqueous carboxylic acids: comparison between different acids and their salts, *J. Phys. Chem. A* 108 (2004) 3324–3337.

[47] V. Doan, R. Köppé, P.H. Kasai, Dimerization of carboxylic acids and salts: an IR study in perfluoropolyether media, *J. Am. Chem. Soc.* 119 (1997) 9810–9815.

[48] R.G. Greenler, Infrared study of adsorbed molecules on metal surfaces by reflection techniques, *J. Chem. Phys.* 44 (1966) 310–315.

[49] M. Sharma, M. Komiyama, J.R. Engstrom, Observation from scanning tunneling microscopy of a striped phase for octanethiol adsorbed on Au(111) from solution, *Langmuir* 24 (2008) 9937–9940.

[50] B.E. Bent, Mimicking aspects of heterogeneous catalysis: generating, isolating, and reacting proposed surface intermediates on single crystals in vacuum, *Chem. Rev.* 96 (1996) 1361–1390.

[51] C.J. Jenks, C.M. Chiang, B.E. Bent, Alkyl iodide decomposition on copper surfaces:  $\alpha$ -elimination and  $\beta$ -hydride elimination from adsorbed alkyls, *J. Am. Chem. Soc.* 113 (1991) 6308–6309.

[52] C.J. Jenks, B.E. Bent, F. Zaera, The chemistry of alkyl iodides on copper surfaces. 2. influence of surface structure on reactivity, *J. Phys. Chem. B* 104 (2000) 3017–3027.